Theor Chem Acc (2006) 116: 316–325
DOI 10.1007/s00214-005-0066-0

REGULAR ARTICLE

M. Elstner

The SCC-DFTB method and its application to biological systems

Received: 13 April 2005 / Accepted: 28 September 2005 / Published online: 23 December 2005

Abstract The Self-consistent charge density functional tight-binding (SCC-DFTB) is an approximate quantum chemical method derived from density functional theory (DFT) based on a second-order expansion of the DFT total energy expression. Here, we review in detail the application of SCC-DFTB to biological systems and several extensions of the original formalism. The biological systems discussed turn out to be a challenge for DFT due to the occurrence of weak binding forces and charge transfer problems, both of which are not properly described by recent DFT-GGA functionals. Possible solutions and alternative strategies are presented and the role of SCC-DFTB in a general quantum chemical approach to biological systems is discussed.

Keywords DFT · SCC-DFTB · Dispersion interaction · QM/MM · Excited states · TD-DFT · Hydrogen bonds · Proton transfer

1 Introduction

The self-consistent charge density functional tight-binding [1] (SCC-DFTB) is an approximate method, which is derived from density functional theory (DFT) by neglect, approximation and parametrization of interaction integrals. It can be viewed as an extension of the original non-self-consistent DFTB [2] method, which is based on an optimized LCAO basis set [3,4] and integral approximations, proposed in earlier work [5]. DFTB is one variant of the tight-binding (TB) family, which found its theoretical justification on the basis of DFT [6] (a recent review discusses the manifold of TB methods including DFTB [7]).

M. Elstner
Deptartment of Theoretical Physics,
University of Paderborn, D-33098 Paderborn, Germany
Deptartment of Molecular Biophysics,
German Cancer Research Center,
D-69115 Heidelberg, Germany
E-mail: m.elstner@dkfz-heidelberg.de

SCC-DFTB (hereafter abbreviated with DFTB) constitutes an alternative to the traditional semi-empirical (SE) methods in Quantum Chemistry like the popular MNDO, AM1 and PM3 schemes, which are derived from Hartree–Fock (HF) theory. Formally, it has some similarity with extended Hückel or CNDO theory, focussing on the matrix elements it exhibits a stronger similarity with the Fenske–Hall Scheme. However, DFTB is not a semi-empirical method in a strict sense, since its parametrization procedure is completely based on DFT calculations, no fit to empirical data has to be performed. In contrast to most SE methods DFTB is a non-orthogonal method, that is, it is based on a non-orthogonal basis set. In the framework of TB theory, this has been emphasized to be a key factor for transferability [7]. Transferability denotes the ability of a parametrized method to perform sufficiently well also for chemical environments not included in the parametrization procedure (SE methods have also been extended to non-orthogonality in the OMx suite of methods [8,9]).

The descent of DFTB from DFT (GGA) is apparent in the description of molecular systems. DFTB often resembles DFT characteristics like the size of the single particle (Kohn–Sham) energy gap (which is usually smaller compared to ab initio methods), or the DFT tendency to underestimate reaction barriers, in particular proton transfer barriers (which are usually overestimated at the HF level of theory). Roughly speaking, DFTB gives results closer to the DFT ones whenever there is a difference with respect to ab initio methods. Of course, problems of the current DFT functionals (GGAs) are also inherited, like the overpolarization in conjugated systems [10] which leads for example, to an underestimation of the bond alternation and the related problem in the description of ionic and charge transfer excited states, or the neglect of dispersion forces.

Till now, DFTB has been applied mostly to solid state and cluster physics [11,12]. The challenges of bio-systems, the large number of atoms and high structural flexibility, which require the treatment of large system sizes and long sampling times in combination with the need for a reliable description of weak binding forces (vdW and H-bonding), and the

complicated potential energy surfaces of bio-molecules made the way to a routine application of DFTB more laborious, which has been partly reviewed recently [13,14].

To cope with extended systems, DFTB has been implemented into linear scaling (O(N)) [15,16] and combined quantum mechanical molecular mechanical (QM/MM) schemes with the force fields AMBER [17], CHARMM [18], TINKER [16] and Sigma [19]. Regarding molecular properties, it has been extended to calculate NMR chemical shifts [20], IR and Raman spectra [13,21–23], excited energy states [24–26] and gradients [26,27] and the conduction through molecules based on Greens Function techniques [28].

DFTB is comparable in computational speed with the SE methods, the main cost is the solution of the generalized eigenvalue problem in a minimal basis, no integrals have to be evaluated during the run-time of the program. SE methods are roughly 2–3 orders of magnitude faster than standard DFT calculations using a DZP basis set. Since matrix diagonalization is an $O(N^3)$ process (N being the number of electrons in the system) and integral evaluation with efficient algorithms becomes $O(N)$ for large systems, the efficiency of SE methods (compared with DFT and HF methods) is largely based on the usage of a minimal basis. Roughly three orders of magnitude higher efficiency allows for ten times larger system sizes [with standard $O(N^3)$ diagonalization] or 1,000 times longer MD sampling, that is, MD simulations in the ns regime become easily feasible. This is an essential ingredient for a reliable determination of the free energies for biomolecular reactions (see also the contribution of Q. Cui in this issue).

To supply useful information concerning biochemical reactions, computational methods have to provide (1) the possibility of sufficient sampling (i.e. have to be computationally very efficient) and have to be (2) accurate in the description of the chemical reaction of interest. While the first requirement overextends the capability of ab initio and DFT methods and leads to the use of SE methods, the second one also is not always complied by DFT, very often more accurate methods are necessary (see, e.g. the discussion of proton transfer reactions that follow). In the previous years, a revival of fast SE methods became apparent due to the requirements of sampling in solution- and biochemistry, while post-HF methods became surprisingly efficient using localization procedures like in the local MP2 and local coupled cluster approaches.

To meet both requirements (1) and (2), the efficiency of SE methods has to be combined with the accuracy of post-HF (or when applicable DFT) schemes. This can be achieved in the so called dual level procedures [29,30] (where the reaction path is calculated with a fast SE method and is then refined at a higher level). Another promising route to an accurate description of biomolecular reactions is a combination of QM methods as in the ONIOM [31] type methodology or in non-additive QM/QM methods [32]. A third possibility is to specifically parametrize SE methods for a certain type of reaction. Transferability requires a high flexibility of the computational method to incorporate various environments, a quality, which definitely is limited in SE methods (and DFTB). Adjusting parameters of SE methods to certain chemical environments in the so called special reaction parametrizations (SRPs) [33] may allow for an accuracy for a specific chemical reaction, which can even be better than that at the DFT or HF level, at the cost of impeding transferability. However, the requirement of long sampling times combined with high accuracy for that specific reaction allows for a reliable treatment of the particular system.

In the following, we describe the theoretical basis of DFTB briefly and then focus on its possible improvements, extension, successes and failures with respect to recent biomolecular applications.

2 Method

SCC-DFTB [1] is derived from DFT by choosing a reference density ρ_0 as a superposition of neutral atomic densities ρ_0^α, $\rho_0 = \sum_\alpha \rho_0^\alpha$ and expanding the DFT exchange-correlation energy functional upto the second order to obtain ($\int d\vec{r}'$ is expressed by $\int'$):

$$E = \sum_i^{\text{occ}} \langle \Psi_i | \hat{H}_0 | \Psi_i \rangle - \frac{1}{2} \iint' \frac{\rho_0 \rho_0'}{|\vec{r} - \vec{r}\,'|} + E_{xc}[\rho_0] - \int V_{xc}[\rho_0]\rho_0 + E_{ii} + \frac{1}{2} \iint' \left(\frac{1}{|\vec{r} - \vec{r}\,'|} + \left. \frac{\delta^2 E_{xc}}{\delta\rho\, \delta\rho'} \right|_{\rho_0} \right) \delta\rho\, \delta\rho'. \quad (1)$$

Equation (1) is the starting point for further approximations leading to the SCC-DFTB model (for details, please see [1]):

(1) The charge density fluctuation $\delta\rho = \rho - \rho_0$ in the second-order term is represented by atomic components, $\delta\rho = \sum_\alpha \delta\rho_\alpha$, and the $\delta\rho_\alpha$ are approximated (using a multipole expansion) by atomic charge fluctuations $\Delta q_\alpha = q_\alpha - q_\alpha^0$, which are computed via a Mulliken charge analysis. The integral over the 1/r term and the second derivative of E_{xc} is approximated by a function γ, which depends on the Hubbard parameter U_α (or chemical hardness η_α), leading to a second-order term:

$$E^{2\text{nd}} = \frac{1}{2} \sum_{\alpha\beta} \gamma_{\alpha\beta} \Delta q_\alpha \Delta q_\beta, \quad (2)$$

where $\gamma_{\alpha\beta} = \gamma_{\alpha\beta}(U_\alpha, U_\beta, R_{\alpha\beta})$ and $U_\alpha = \frac{1}{2} \frac{\partial^2 E_{\text{at}}}{\partial q_{\text{at}}^2}$ is the second derivative of the energy of the atom α with respect to its total charge.

(2) The Kohn–Sham orbitals Ψ_i are expanded in an optimized LCAO basis set ϕ_μ as suggested by Eschrig and Bergert [3], $\Psi_i = \sum_\mu c_\mu^i \phi_\mu$. This minimal basis set, consisting of slightly compressed atomic orbitals, which are determined

by solving the atomic Kohn-Sham problem in an additional confining potential [2]

$$[T + v_{\text{eff}}(\rho) + \left(\frac{r}{r_0}\right)^2]\phi_\mu = \epsilon_\mu \phi_\mu, \tag{3}$$

has been shown to represent the molecular density better than uncompressed atomic orbitals [5]. Originally, these optimized orbitals were determined by treating r_0 as a variational parameter in DFT SCF calculations [3,4]. In the SCC-DFTB framework, r_0 is chosen to be twice the covalent radius and can be further optimized. Similarily, the initial density ρ_0^α is determined using a different confining radius r_0^d. While the determination of r_0 can be compared with the optimization of basis sets for DFT calculations, r_0^d can be regarded as an empirical parameter as suggested by the work of Foulkes and Haydock [6]. They showed, that the TB methodology can be understood as an approximation to DFT, critically depending on the choice of an appropriate input density. The input density ρ^0 has to be optimized in order to minimize the error of the TB total energy with respect to the true ground state energy. Within DFTB, both confining radii usually have a limited influence on molecular properties of interest. Therefore, the process of choosing the confining radii cannot be compared with the optimization procedure in semi-empirical MO theory, where parameter determination is performed by a 'brute force optimization' in a multidimensional parameter space. $\rho_0 = \sum_\alpha \rho_0^\alpha$ and ϕ_μ enter the calculation of the Hamilton matrix elements in the AO basis [first term on the rhs of Eq. (1)]

$$\hat{H}^0_{\mu\nu} = < \phi_\mu | \hat{H}(\rho_0) | \phi_\nu >, \tag{4}$$

where we neglect the so called crystal field terms when calculating the diagonal elements as $H^0_{\mu\mu} = \epsilon_\mu$ with ϵ_μ being the Kohn–Sham eigenvalue of the neutral, unconfined atom. The non-diagonal elements are evaluated in a two-centre approximation, $\hat{H}^0_{\mu\nu} = < \phi_\mu | \hat{H}(\rho_0^\alpha + \rho_0^\beta) | \phi_\nu >$ thereby neglecting three-centre terms. The latter approximation is justified by the early observation that the three centre terms and the core orthogonalization integrals tend to cancel. The Hamilton $\hat{H}^0_{\mu\nu}$ and overlap $S_{\mu\nu} = < \phi_\mu | \phi_\nu >$ matrix elements are calculated for interatomic distances on a relevant scale and are tabulated. Therefore, the dominant computational cost is the solution of the generalized eigenvalue problem for the charge self-consistent Hamiltonian

$$\hat{H}_{\mu\nu} = \hat{H}^0_{\mu\nu} + \frac{1}{2} S_{\mu\nu} \sum_\gamma \Delta q_\gamma \left(\gamma_{\alpha\gamma} + \gamma_{\beta\gamma}\right). \tag{5}$$

(3) Finally, the term defined as E_{rep},

$$E_{\text{rep}} = -\frac{1}{2} \iint' \frac{\rho_0' \rho_0}{|\vec{r} - \vec{r}\,'|} + E_{xc}[\rho_0] - \int V_{xc}[\rho_0] n_0 + E_{ii} \tag{6}$$

is approximated as a sum of two body potentials (for a more detailed description, see e.g. [6])

$$E_{\text{rep}} = \sum_{\alpha\beta} U_{\alpha\beta} \tag{7}$$

Finally, the approximate DFTB total energy reads as:

$$E_{\text{tot}} = \sum_{i\mu\nu} c^i_\mu c^i_\nu H^0_{\mu\nu} + \frac{1}{2} \sum_{\alpha\beta} \Delta q_\alpha \Delta q_\beta \gamma_{\alpha\beta}(R_{\alpha\beta}) + E_{\text{rep}} \tag{8}$$

In practice, $U_{\alpha\beta}$ is fitted as the difference of total energies from DFT and the electronic part of DFTB with respect to the bond length of certain bonds in reference molecules. For example, to calculate $U_{\alpha\beta}$ for the C–C interaction, we calculate the DFT and DFTB electronic energies by stretching and compressing the C–C bonds of H_3CCH_3, H_2CCH_2 and HCCH around their equilibrium bond lengths and combine the resulting energy curves. This step of the parametrization is the most time consuming one, since the determination of the pair potentials constitutes an N^2 effort within the periodic table. Figure 1 shows the DFT total energy curve (solid line), where the respective contributions from HCCH between about 2.1 and 2.35 a.u., from H_2CCH_2 between about 2.35 and 2.65 a.u. and from H_3CCH_3 for distances larger than 2.65 a.u. are combined into one curve. Note that the respective DFT total energy curves are shifted in order to obtain one continuous curve. The same is done for the SCC-DFTB electronic part [first two terms on the rhs of Eq. (8)]. Again, the respective parts are shifted in order to obtain an overall continuous energy versus bond distance curve. $U_{\alpha\beta}$ is then calculated pointwise as the difference of the DFT and DFTB energy curves and fitted by splines (or polynomials). This procedure results in an analytical representation of $U_{\alpha\beta}$, which is continuous also in its first and second derivatives. For other atom pairs, the same strategy is used. For example, to calculate $U_{\alpha\beta}$ for C–O, the molecules H_3COH, H_2CO and CO were used, for the parametrization of C–H only CH_4, for sulphur see Ref. [34] and for zinc see [35].

In the whole parametrization procedure, no reference to empirical data is made, that is, every step is based on DFT calculations. For every atom pair (e.g. C–C or C–N), at most two or three molecules are used for the parametrization. The main point is to include information from the equilibrium

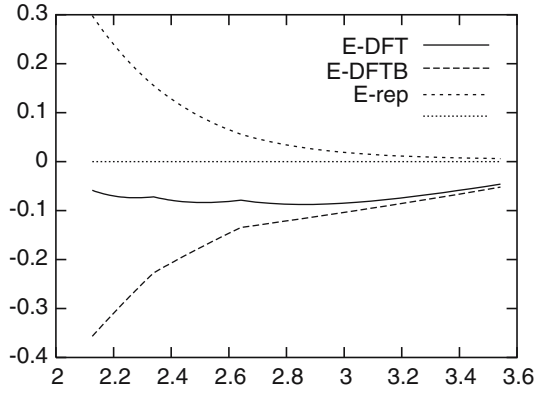

Fig. 1 *E-DFT* shows the (shifted) total energy versus C–C distances (in a.u.) for HCCH, H_2CCH_2 and H_3CCH_3, E-DFTB the same for the electronic part [first two contributions in Eq. (8)] of DFTB total energy. *E-rep* is the difference of this two curves

distances of single, double and triple bonds. This usually ensures a good description in other bonding situations, for example, for the partial double bonds in benzene or fullerenes. Of course, an extension to cover transition states is also possible.

In a first version, the DFTB parameters were calculated using a LDA functional [2] and SCC-DFTB has been tested in detail for reaction energies, geometries rotational and proton transfer barriers for a large set of small organic molecules [36]. Using the PBE functional as the basis for parametrization [1], in particular reaction energies could be improved significantly. For 28 reactions we found a mean average deviation from the G2 results of 4.3 kcal/mole [37]. Several reactions, however, show deviations of up to 12 kcal/mole, while geometrical parameters are in excellent agreement with ab initio data [34,36,37]. The most severe shortcoming is DFTB's inability to describe the dihedral angel in hydrogen peroxide. For the investigated vibrational frequencies of 22 molecules, DFTB shows a 75 cm^{-1} mean absolute deviation from the reference values [37]. Another study using a larger set of 66 molecules containing O, N, C, H and S atoms found an error (mean absolute deviation) of 57 cm^{-1} [38]. While vibrational frequencies are described quite well for many important vibrational modes, some of them exhibit substantial errors, for example, the C=C double bond stretch and the NH modes are severely overestimated [36–39]. The main emphasis during the parametrization for Zinc laid on the description of biologically relevant chemical situations, therefore, the DFTB parametrization has been tested in great detail for ligand-binding energies, proton affinities and geometries of a large set of Zinc containing compounds [35], a strategy, which is also used in the development of parameters for Copper and further transition metals.

3 Improving accuracy

Approximate methods utilizing a minimal basis set like the SE quantum chemical methods or DFTB are limited in their flexibility to represent various chemical environments with appropriate accuracy, however, their main advantage is a very good computational cost versus accuracy ratio. Therefore, strategies to improve the accuracy should try not to sacrifice the computational efficiency significantly since this may shrink the advantage over very efficient DFT-GGA implementations like the SIESTA [40] or QICKSTEP [41] program packages.

(1) Obviously, one can go beyond the second-order approximation by including the third-order term:

$$E^{3\mathrm{rd}} = \frac{1}{6}\iiint''' \left(\frac{\delta^3 E}{\delta\rho\,\delta\rho'\,\delta\rho''}\bigg|_{\rho_0} \right) \delta\rho\,\delta\rho'\,\delta\rho''. \tag{9}$$

Applying the same approximations as for the second-order term [1], we can derive a simple third-order extension to SCC-DFTB by keeping one-centre contributions only

$$E^{3\mathrm{rd}} = \frac{1}{6}\sum_{\alpha} \frac{\partial U_\alpha}{\partial q_\alpha} \Delta q_\alpha^3. \tag{10}$$

The Hubbard derivative can be evaluated in the following way: Hubbard parameters are calculated for various charge states of the atom and fitted to a first order polynomial. The numerical derivative of this resulting curve is taken as Hubbard derivative. This approximation takes into account the (linear) charge dependence of the Hubbard parameter, which may be important for highly charged species, since the hardness of an atom is expected to change with its charge state. This extra term turns out to be of particular importance for more accurate proton affinities as discussed next. It should be emphasized, that this extension does not improve the performance of DFTB in general, but only when large charge transfer within the molecular systems becomes important.

A second extension regarding the charge-dependent term consists in the use of a different scheme to evaluate the atomic charges Δq_α. Recently, Kalinowski et al. [42] have implemented the CM3 scheme from Cramer and Truhler into DFTB with great success. The molecular charge distribution and also the molecular dipole moments are much improved. However, the influence on other properties like reaction energies, geometries or vibrational frequencies is expected to be small.

Third, one can optimize the γ function used to interpolate between the cases $R_{\alpha\beta} \to \infty$ and $R_{\alpha\beta} = 0$. In SE theory, several choices for the coulomb interaction are used, one of them being the so called Klopman–Ohno scaling

$$\gamma_{\alpha\beta} = \frac{1}{\sqrt{R_{\alpha\beta} + 0.25\left(1/U_\alpha + 1/U_\beta\right)^2}}, \tag{11}$$

or the Mataga–Nishimoto scaling

$$\gamma_{\alpha\beta} = \frac{1}{R_{\alpha\beta} + 0.5\left(1/U_\alpha + 1/U_\beta\right)}, \tag{12}$$

γ in DFTB has a quite similar curve shape, being slightly more repulsive in the covalent binding region than the function of Klopman–Ohno. However, it is more complicated in its functional form and consists of an $1/R_{\alpha\beta}$ part and an exponentially decaying short range part $S_{\alpha\beta}$ [1],

$$\gamma_{\alpha\beta} = 1/R_{\alpha\beta} - S_{\alpha\beta}. \tag{13}$$

$S_{\alpha\beta}$ describes the deviation of $\gamma_{\alpha\beta}$ from the $1/R_{\alpha\beta}$ behaviour with increasing overlap of α and β and is responsible for the convergence of $\gamma_{\alpha\beta}$ to a finite value at zero distance. The determination of $\gamma_{\alpha\alpha}$ as U_α implies that the extension of the atomic charge density and its chemical hardness are inversely proportional [1]. While this holds approximately for the second and third-row elements, hydrogen deviates substantially from this behaviour. To account for this, we allow $\gamma_{\alpha\beta}$ to deviate from the given functional form when hydrogen is involved (i.e. for X–H interactions, X=heavy elements) by introducing an additional term $f(_{\alpha\beta})$:

$$\gamma_{\alpha\beta} = 1/R_{\alpha\beta} - S_{\alpha\beta} * f(_{\alpha\beta}). \tag{14}$$

By damping the short-range term, $\gamma_{\alpha\beta}$ becomes more repulsive especially in the region of covalent binding (1 − 2 Å). This leads to a larger polarization of the respective (polar) bond, which turns out to improve hydrogen bonding in particular.

Fourth, one could improve the description of the second-order term by going beyond the monopole approximation of the charge density fluctuations on atoms α, $\delta\rho_\alpha$ for example, by accounting for dipole–dipole interactions as for example, in the MNDO framework [43]. Till now, no attempts have been made in this regard.

(2) One obvious extension is to improve the basis set, that is, to augment it with a second set of valence and polarization functions. In some cases, like sulphur [34] and phosphorus, inclusion of polarization functions is necessary, in particular to describe the hypervalent species. The use of polarization functions on hydrogen to improve hydrogen bonding is successful in principle [13], but not recommended due to the significant increase of the computational cost. Due to the same reason the use of split valence basis sets, although possible in principle, has been avoided till now. The computational cost would increase by nearly one order of magnitude when going to a double zeta basis. Clearly, this decision limits its DFTB accuracy in several ways, for example, it reduces the molecular polarizability [32] and probably also the Pauli repulsion in intermolecular interactions, which leads to the small intermolecular distances in hydrogen-bonds [13] and stacked complexes [44], and probably leads to an overestimation of the strain energy in small ring molecules [37].

The neglect of the so called crystal field terms for the computation of the diagonal matrix elements and the three-centre terms may be a further factor reducing DFTBs flexibility to respond to different environments. Here, in particular highly coordinated phases may be treated insufficiently, as has been shown in an extension of a TB method by including these terms [45]. The neglect of these terms in DFTB is not due to the computational cost, but due to the highly sophisticated problem of finding a balanced description without running into a prevalent parametrization effort.

(3) There are several choices for the treatment of E_{rep}: first, one could compute it from first principles and tabulate in a similar way as the matrix elements. However, the parametrization of E_{rep} with respect to DFT calculations probably leads to a higher accuracy. The fitting procedure of E_{rep} could be made much more sophisticated, in particular by taking more information into the data set, that is, not only equilibrium geometries but also transition state structures. This again, however, may increase the fitting effort substantially.

Therefore, there are several ways to improve DFTB while maintaining its efficiency. Also a basis set extension is an option, however, less favoured. E_{rep} is definitely the term, which can be changed most easily and is an ideal candidate for improving DFTBs performance for specific chemical environments, that is, for a SRP. This has been done successfully, for example, to improve DFTBs description of geometries and vibrational frequencies [22].

4 Description of biological structures

The strenght of DFTB is definitely its accuracy for geometries of even larger structures. It has been successfully applied to peptides, yielding very good structures and relative energies for the various conformations in this complex energy landscape [46–48]. Interesting insight into the dynamics of peptides and proteins has been obtained by long timescale MD within QM/MM and O(N) QM/MM implementations in comparison with classical forced fields [16,19].

DFTB gives a good description of DNA base geometries as well [49], and also reproduces the sugar puckering. This allows its application to questions related to DNA and DNA-intercalator interactions [50–53], after being augmented with empirical dispersion.

The protonated Schiff base retinal (pSB) is a polyene chain, which is linked to the protein backbone via a protonated Schiff base and acts as the chromophore in the familiy of retinal proteins. This molecule has a quite complicated electronic structure, which is a challenge to computational chemistry, since exchange and correlation effects have to be included for a balanced description. DFTB has been shown to describe ground state properties of pSB (bond length alternation of the polyene chain, torsional barriers, and so on) with an accuracy comparable with the full DFT methods, being about three orders of magnitude faster [54]. Since this ligand is difficult to parametrize for empirical force fields, DFTB has been used in QM/MM algorithms to calculate optimized geometries and MD trajectories [55], which were the basis for the calculation of retinal absorption energies [56]. Recently, it has been successfully applied to refine the rhodopsin crystal structure [57].

5 Adding empirical dispersion to DFT

In principle, DFT yields the exact ground state density, which also includes the long range vdW forces however, it has been recognized quite early that common LDA and GGA functionals do not account for dispersion forces [58–60], in particular for the long range component ($C_6 R^{-6}$ and higher contributions). As has been shown for the interaction of rare gas dimers, several GGAs result in purely repulsive interactions, while others like PW91 and in particular LDA lead to attractive interactions, however, largely overestimating [58, 60–63] interaction energies. Clearly, current GGA functionals cover only the short ranged (overlap dependent), exponentially decaying, contribution [58,62] to the dispersion energy. However, this is covered very differently by the various GGA functionals [62,64]. Moreover, although the exchange part should be purely repulsive for rare gas dimers, the magnitude of repulsion varies with the functional, which can be traced back to their different behaviours at the small density and high reduced gradient region [61,65]. GGAs can lead even to an artificial (wrong) attraction at the exchange only level (PW91) [63]. Different GGA functionals seem to behave very different in both their exchange and correlation parts [66], thereby, possibly overestimating Paul repulsion (B88) or artificially leading to attraction (PW91 exchange) [63] and cover correlation effects due to the short range overlap term in varying degrees [62].

Further, although DFT performs quite well for hydrogen bonding in general, deficiencies in the description of the angular dependence of the GGA potential energy surfaces have been reported, probably again due to the missing dispersion interaction [67–69].

A simple combination of existing functionals may balance the individual parts of exchange and correlation in a better, but completely empirical way [70–72], that is, may lead to a compensation of artificial attraction of PW91 and excessive repulsion of B88, however, will not solve the problem of the missing long range contribution. Modifications of PBE, xPBE [74] and revPBE [75,76] seem to lead to a balanced treatment of the short range part of dispersion and exchange repulsion, as already indicated by the behavior of the enhancement factor in the large gradient limit. However, this does not lead to a satisfactory description of vdW complexes, since for example, DNA base pairs are definitely not bound at the GGA level even using PW91 (which overbinds the rare gas dimers) [73], that is, the long range part of dispersion, which is not in the region of overlap effects is definitively missing. A similar conclusion has been drawn recently from a study of molecular crystals [77].

Approaches to calculate the long range parts from DFT have been suggested either by calculating the monomer polarizabilities at imaginary frequencies [78,79] or through DFT SAPT theory [80–82], both approaches, however, are not applicable for intramolecular dispersion effects. There are various attempts to construct functionals including an appropriate long range part, as can be found for example, in Refs. [76,83–85].

Another route to include the vdW interactions is by empirically adding them in the spirit of the HF+dispersion (HFD) calculations several decades ago [86] (revisited, e.g by Ref. [87]). Recently, a post-Hartree–Fock model for the dispersion interaction [88,89] has been proposed.

In principle, this procedure can be also applied to DFT, however, in this case a double counting of correlation contributions in the overlap region will be introduced. Therefore, the damping function, which in HFD has the task to avoid artificial singularities becomes peculiar in the case of DFT. The problem of double counting cannot be avoided but only be empirically taken care of by designing the damping function and the empirical C6 parameters in order to reproduce a large set of reference data.

Adding empirical dispersion with a special choice of a damping function $f(R_{\alpha\beta})$ (which rapidly approaches zero for short distances),

$$E = E_{\mathrm{DFTB}} - \sum_{\alpha\beta} f(R_{\alpha\beta}) \frac{C_{\alpha\beta}}{R_{\alpha\beta}^6}, \tag{15}$$

and empirical $C_{\alpha\beta}$ coefficients worked in DFTB rightaway, when comparing DNA base pair stacking energies with those from MP2 [44]. This good agreement is confirmed for an extended set of stacked molecules by comparing with coupled cluster results (to be published). As mentioned previously, intermolecular distances are underestimated in general, probably due to underestimation of overlap repulsion within the minimal basis set.

Obviously, dispersion is crucial for DNA base pair stacking and interaction of bases with intercalators and DFTB + dispersions have been applied successfully in a couple of studies to these problems [50–53]. Interestingly, dispersion is also crucial for the conformations and relative energies of peptides and proteins. Without dispersion, proteins may be instable and relative energies of various polypetide conformations are largely in error (for a review, see Ref. [14]), showing the need for current DFT functionals to be augmented with empirical dispersion before being applied to biological problems.

Augmenting full DFT with empirical dispersion in the same way, leads to results which are dependent on the DFT functional and damping function used [63,90,91], since both, C6 coefficients and the damping function should be calibrated in order to account for the double counting. The different amounts to which GGAs cover both Pauli repulsion and dispersion within the overlap regime have to be taken into account as for example, in the work of Grimme [92]. Grimme scaled the dispersion energy by 0.7 when adding it onto PBE, thereby accounting for the fact that PBE (similar to PW91) is too attractive at the exchange only level already, and by scaling by 1.4 when using BLYP, taking into account the excessive Pauli repulsion of the B88 exchange functional (the scaling factors were the subject of optimization with respect to a large data set). Probably one of the functionals like XLYP, revPBE, where Pauli repulsion and dispersion in the overlap region are covered in a more balanced way, is even a better starting point for augmenting with empirical dispersion.

6 Excited states and DFT(B)

Within DFT, the most promising route to excited states of molecules is via the time-dependent DFT (TDDFT) response formalism, which is already implemented into various DFT codes and is now increasingly used. Therefore, we have implemented this formalism also within the framework of our SCC-DFTB method [24], showing reasonable results for excited state energies when compared with the full TDDFT results (and exhibiting the same problems, as discussed next).

To compute excited state energies in the TDDFT framework, in addition to the Kohn–Sham energy differences $\omega_{ij} = \epsilon_j - \epsilon_i$ the so called coupling matrix

$$K_{ij\sigma,kl\tau} = \int\int \Psi^{i\sigma}(\mathbf{r})\Psi^{j\sigma}(\mathbf{r}) \left(\frac{1}{|\mathbf{r}-\mathbf{r}'|} + \frac{\delta^2 E_{xc}}{\delta\rho_\sigma(\mathbf{r})\,\delta\rho_\tau(\mathbf{r}')} \right) \Psi^{kj}(\mathbf{r}')\Psi^{lj}(\mathbf{r}')\mathrm{d}\mathbf{r}\mathrm{d}\mathbf{r}' \tag{16}$$

has to be evaluated, which leads to the excitation energies ω_{I} after solving the eigenvalue problem

$$\sum_{ij\sigma} \left[\omega_{ij}^2 \delta_{ik}\delta_{jl}\delta_{\sigma\tau} + 2\sqrt{\omega_{ij}} K_{ij\sigma,kl\tau} \sqrt{\omega_{kl}} \right] F_{ij\sigma}^I = \omega_I F_{kl\tau}^I. \tag{17}$$

The main difference between the integral in Eq. (16) and the second-order term in Eq. (1) is that the second derivative is not taken at ρ_0 and that the integral contains the transition density $\Psi^i(\mathbf{r})\Psi^j(\mathbf{r})$ instead of the density $\rho(\mathbf{r})$. Similar to the approximation of the second-order term in Eq. (1), we apply a monopole approximation to the transition density leading to the transition charges on atom α, $q_\alpha^{ij} = \sum_{\mu\epsilon\alpha}\sum_\nu \frac{1}{2}\left(c_\mu^i S_{\mu\nu} c_\nu^j + c_\mu^j S_{\mu\nu} c_\nu^i\right)$ and approximate the second derivative again with the $\gamma_{\alpha\beta}$ function described previously.

$$K_{ij\sigma,kl\tau} = \sum_{\alpha,\beta} q_{ij}^\alpha \left[\gamma_{\alpha\beta} + (2\delta_{\sigma\tau} - 1)m_{\alpha\beta}\right] q_{kl}^\beta, \tag{18}$$

where $m_{\alpha\beta}$ is calculated from the second derivative of E_{xc} with respect to magnetization. The various approximations involved including that of using a minimal basis set of course leads to a loss of accuracy with respect to full DFT, however, the formalism is several orders of magnitude faster than full DFT [24]. TD–DFTB has been benchmarked with respect to TDDFT for a set of small organic molecules [24,25].

Although many successful and promising applications of TDDFT in Physics and Chemistry have been reported, Biology seems to favour chromphores, which bring current GGA functionals to their limits. Commonly occurring molecules like polyenes (β-carotenoids) or porphyrenes exhibit strongly ionic excited states, which have been shown to be described quantitatively wrong using TDDFT [93] and even qualitative failures have been reported when studying the excited states of potential energy surfaces [26]. This is connected to observations of other groups, describing deficiencies of DFT with respect to polarizabilities of conjugated chains [10]. The situation is even worse, when considering intermolecular [95,96] or intramolecular charge transfer excitations [26]. Applying these methods to retinal absorption energies, dramatic failures have been found. In particular, the wrong asymptotic description of charge transfer (CT) excitations is related to the local character of the DFT XC kernel [26,95,96].

New developments in non-local (orbital dependent) XC functionals [98] may provide a solution to these problems and we are currently testing several options within the SCC–DFTB framework.

A different route to incorporate many body effects into the calculations of DFT excitation energies is followed in the GW [97] and Bethe–Salpeter equations, which are currently implemented into DFTB.

Because of the problems of current DFT functionals with CT systems, we tested the semi-empirical OM2 method in combination with the MRCI algorithm [9,100] and the newly developed ab initio MRCI method SORCI [101]. We assessed the performance of these and other, currently used, computational approaches to accurately model changes in absorption energies with respect to changes in geometry and applied external electric fields [56]. In this article we illustrate the high sensitivity of absorption energies on the ground state structure of retinal, which varies significantly with the computational method used for geometry optimization. The response to external fields, in particular to point charges, which model the protein environment in combined QM/MM applications, is a crucial feature, which is not properly rendered by previously used methods, such as TDDFT, complete active space self-consistent field (CASSCF), and HF or SE configuration interaction singles (CIS). This is discussed in detail for the example of bacteriorhodopsin (bR), a protein which blue-shifts the retinal gas phase excitation energy by about 0.5 eV [56].

The combination of SCC-DFTB QM/MM optimized geometries with SORCI QM/MM excited state calculations leads to a bR excitation energy of 2.34 eV being close to the experimental value of 2.18 eV.

As a result of this study, we propose a combination of the fast DFTB method for computing QM/MM ground state optimized geometries or MD trajectories and OM2/MRCI and SORCI for calculation of excitation energies as a promising route to study optical properties in various photoproteins. A first successful application to the problem of colour tuning shows that computational approaches have the capability to reproduce the experimental data regarding mutation experiments and can lead to a mechanistic explanation of the structural determinants of optical properties of photoproteins.

7 DFTB and Hydrogen bonds

Hydrogen bonding energies are largely overestimated in DFT-LDA, however, a much better description is given with GGA functionals. The BLYP and B3LYP functionals slightly underestimate hydrogen bond strengths, while PBE seems to slightly overestimate them (see, e.g. Ireta et al. [69] and references therein). Problems in describing the angular dependence of hydrogen bonding properly may be related to the deficiency with respect to dispersion interactions at the GGA level, as mentioned above [67–69].

DFTB describes hydrogen bonds quite well in terms of structures, thereby slightly underestimating the hydrogen bonding distances by about 0.1 Å on average, again, probably due to the underestimation of Pauli repulsion within the minimal basis set. Also, hydrogen bonding energies are systematically underestimated by about 1–2 kcal/mole [13, 17,44,102].

To improve the description of DFTB hydrogen bonds, three possibilities exist, each by modifying one of the three terms in the DFTB total energy expression Eq. (8).

One option is to modify the E_{rep} term by effectively introducing an artificial minimum in the X–H (X: S, O, N, C) potentials at the corresponding hydrogen bonding distance, thereby, increasing the interaction energy to the desired hydrogen bond strength. This can be compared with the strategy of the MNDO/M model [103], where hydrogen bonding in MNDO was improved by modifying the core–core repulsion. We tried this option and it is moderately successful, the overall description can be improved, that is, the systematic underestimation of hydrogen bond strengths can be removed (data not shown). However, the resulting model is not very

flexible, for example, it is not able to properly account for cooperativity in hydrogen bonding (e.g. in water clusters). This is no surprise since cooperativity cannot be covered by simple two-body potentials, and, related to that, the description of strong hydrogen bonded complexes is not satisfactory.

A second option is to modify the term containing the Hamilton Matrix $H^0_{\mu\nu}$ in Eq. (8). The main effect may be gained by increasing the basis set, rather than by improving the integral approximations. Therefore, we have added polarization functions to the hydrogen atoms, as suggested by Jug and Geudtner [104] for the SINDO1 model. The resulting hydrogen bonding energies and geometries look very promising [13], however, at the expense of an increasing computational cost. Adding p functions on hydrogens nearly doubles the basis set size for biological molecules (assuming the systems to consist of 50% hydrogen atoms and 50% heavy atoms), therefore, leading to a factor of about 8 in the CPU time.

The third option is to modify the second-order term in Eq. (8) as suggested previously by changing the functional form of γ. By choosing an appropriate damping for the short range part in the γ function, an increased interaction in the region of the covalent bond can be obtained, that is, in the region of 1–3 Å where γ deviates from $1/R$. This leads to an increased polarization of the molecule and the increased dipole moment leads to an stronger intermolecular interaction, that is, stronger hydrogen bonds. Since (bio)molecules are on average slightly underpolarized within DFTB, which can be seen for example, for the dipole moments of small peptide fragments [46], the increased coulombic interaction in the modified γ function directly compensates for this shortcomings. This modification does not increase the computational cost and leads to a balanced description of weak and strong hydrogen bonds including cooperativity effects.

The indication, that the lack of dispersion interactions in DFT shows up also for hydrogen bonded systems, suggests to include the empirical dispersion correction for these systems also from the beginning.

8 Proton transfer reactions

The accuracy of computational methods for proton transfer (PT) reactions can be estimated beforehand by looking at two (independent) properties: barrier heights can be studied for model systems like the protonated water dimer or malondhyde, the accuracy for reaction energies can be estimated from gas phase proton affinities and deprotonation energies of the donor and acceptor molecules (or models).

Pure DFT (GGA) functionals seem to underestimate the barriers substantially, while HF overestimates them largely [114,115]. Both methods, therefore, are not appropriate for studying proton transfer reactions. Due to error compensation, the hybrid B3LYP functional tends to reproduce higher level calculations quite well, as can be seen for example, from the performance for some low barrier transfer systems like $H_7N_2^+$, $H_5O_2^+$ and malondehyde [109,114,115]. When the barrier is low ($\approx$ 5 kcal/mol), B3LYP underestimates PT barriers by about 1–2 kcal/mol, for higher barriers, this error increases to 2–4 kcal/mol (unpublished results). B3LYP may lead to a good estimate of barrier enthalpies due to a further error cancellation: as described in the review of Gao and Truhlar [116], corrections for zero point vibrational energies (ZPE) usually lower PT barriers by about 2–4 kcal/mol. Therefore, neglect of ZPEs may bring B3LYP results into reasonable agreement with experimental data.

DFT seems to be quite reliable with respect to protonation and deprotonation energies [117–119], although differences to higher level calculations of few kcal/mol for specific systems can be found [18,105]. When the proton is bound to an extended conjugated chain like in the protonated Schiff base retinal, considerable errors of DFT can be found due to its tendency to overpolarize these chains [10] and thereby, to overstabilize the extra positive charge along the chain.

Several studies found DFTB PT barrier heights in reasonable agreement with the corresponding values from B3LYP [18,36,109,112], therefore, DFTB tends to underestimate barrier heights as well. For example, our good agreement with experimental results for the PT barrier of the first PT step in bacteriorhodopsin [111,112] may be due to the discussed error cancellation (lower barriers versus ZPE). Therefore, ZPE corrections may be successfully taken into account only at higher levels of theory (MP4 or CCSD). Since geometries at the SCC-DFTB level have been shown to be quite reliable, one could use PT pathways calculated with DFTB refined by higher level single point energies (dual-level approach).

The PT reaction profile in LADH [105] however, shows one of the inaccuracies of the DFTB method, finding an $\approx$ 10 kcal error in the reaction energy of the first PT step. This can be traced back to the inaccuracy of DFTB in describing protonation and deprotonation energies of the involved proton donors and acceptors. One possible solution consists in going beyond the second-order approximation: by including third-order terms, the protonation and deprotonation energies can be significantly improved. For the description of highly charged, most anionic species a dependence of the chemical hardness (Hubbard parameter) on the charge state of the atom seems to become crucial. The effect can be demonstrated for the isolated water molecule: the protonation energy of water evaluated with second-order DFTB is in good agreement with higher level results, and does not change when including third-order terms. The deprotonation energy ($H_2O \rightarrow OH^- + H^+$) is in error by about 40 kcal/mol at the second-order level, reducing to few kcal/mol when including the third-order term. Deprotonation energies of acids (R-COOH) at the secnd-order DFTB are still about 10 kcal/mol in error, reducing to few kcal/mole at the third-order. This behaviour can be found for nearly all anions, going from second-to-third-order DFTB leads to a significant improvement, while the positively charged compounds are already mostly in good agreement with higher level results and do not change upon inclusion of the third order term.

However, specific problems with nitrogen in certain chemical environments, mostly for sp3 nitrogen, could not be

resolved by the third-order terms: here, we found errors of about 10 kcal/mole. We first recognized this problem when investigating intramolecular PT reactions in the DNA bases guanine and uracil, where proton acceptors can be either oxygen or nitrogen. To correct this error, we developed a special parametrization for nitrogen by modifying the N–H repulsive potential to correct for the wrong energetics. This potential has been already applied to the first PT in bacteriorhodpsin, where the proton moves from the nitrogen of the Schiff-base retinal to a nearby aspartate [111,112], and to the PT in carbonic anhydrase.

Hopefully, the third-order extension in combination with the SRP for nitrogen-containing species will provide a methodology, which allows for reliable treatment of PT reactions in biological systems without any need for further SRPs.

9 Conclusion

Although DFTB has been applied successfully to many problems of interest, it should be kept in mind that it is an approximate method with a certain, limited flexibility to adjust to different chemical environments. We have discussed several extensions – from improvements of the DFTB approximation (e.g. third-order expansion) upto ad hoc fixes of DFT failures (dispersion forces)- which do not affect the computational efficiency. Other, more involved improvements like an extended basis set may be incorporated in the near future, however, this would move DFTB out of the "middleground" of computational methods [120], that is, concerning computational efficiency it would come closer to the full DFT methods instead of being in the "middle", between empirical force field and ab initio methods, where SE methods fill an obvious gap.

DFTB has been applied successfully to determine structures and dynamic behaviour of many biomolecules like peptides, DNA and different types of ligands and its use as a high-level method in this context has been discussed recently [14]. In general, DFTB seems to be quite reliable in terms of molecular structures, a requirement for its future use in QM/QM and dual-level schemes. Concerning energetics, vibrational frequencies and properties, we can summarize as follows:

(1) Due to their limited flexibility, SE methods (and DFTB) should be tested before application for every class of structures/reactions independently in comparison with higher level methods. However, due to the problems of DFT (dispersion, CT excitations, PT barriers, transition metals), it is not always a good reference and higher level methods may be a better choice. This is feasible now since computationally cheaper ab initio variants like local MP2 or local coupled-cluster methods are becoming available.

(2) For applications, where the intrinsic accuracy of DFTB is not sufficient it may be combined with higher level methods in various ways: it may be used either as a fast method, which allows for sufficient sampling or to perform the costly reaction path calculations, while the final energetics is improved/corrected at a higher level method by applying dual-level (Truhlar), ONIOM (Morokuma) or QM/QM type methods. A different type of QM/QM combination has been proposed for the determination of IR intensities [18], where geometry and Hessian are calculated with DFTB while the dipole derivatives along the normal modes are calculated with B3LYP, which may be a good compromise between efficiency and accuracy.

(3) Due to the limited flexibility, it may not be possible to achieve the desired accuracy for all desired properties simultaneously. For example, it may not be possible to obtain both, very accurate energetics and vibrational properties, within one parametrization. Therefore, there may be different parameter sets for different purposes, for example, a special parametrization for vibrational frequencies is in progress. Another example is the proton affinity, where it may be necessary to have two sets of N–H parameters, one for the standard applications, the other for studying PT reactions including nitrogen as a donor/acceptor. In principle, it is possible to develop SRPs for certain classes of reactions. This may be a way to combine the requirements of computational efficiency needed for appropriate sampling and inherent high accuracy for the description of the particular reaction of interest.

Acknowledgements I would like to thank G. Seifert, D. Porezag, T. Frauenheim, S. Suhai, T. Niehaus and Q. Cui, who contributed significantly to make DFTB work for biological systems.

References

1. Elstner M, Porezag D, Jungnickel G, Elsner J, Haugk M, Frauenheim T, Suhai S, Seifert G (1998) Phys Rev B 58:7260
2. Porezag D, Frauenheim T, Köhler T, Seifert G, Kaschner R (1995) Phys Rev B 51:12947
3. Eschrig H, Bergert I (1978) Phys Stat Sol B 90: 621
4. Eschrig H (1988) The optimized LCAO method and electronic structure of extended systems. Akademieverlag, Berlin
5. Seifert G, Eschrig H, Bieger W (1986) Z Phys Chem (Leipzig) 267:529
6. Foulkes W, Haydock R (1989) Phys Rev B 39:12520
7. Goringe CM, Bowler DR, Hernandez E (1997) Rep Prog Phys 60:1447
8. Kolb M, Thiel W (1993) J Comp Chem 14:775
9. Weber W, Thiel W (2000) Theoret Chem Acc 103:495
10. Champagne B et al. (2000) J Phys Chem A 104:4755
11. Frauenheim T et al. (2000) Phys Stat Sol B 217:41
12. Frauenheim T et al. (2002) J Phys Condens Matter 14:3015
13. Elstner M et al. (2000) Phys Stat Sol **b** 217:357
14. Elstner M, Frauenheim T, Suhai S (2003) J Mol Struc (THEOCHEM) 632:29
15. Sternberg M, Galli G, Frauenheim T (1999) Comp Phys Comm 118:200
16. Liu H et al. (2001) Proteins 44:484
17. Han W et al. (2000) Int J Quant Chem 78:459
18. Cui Q et al. (2001) J Phys Chem B 105:569
19. Hu H, Elstner M, Hermans (2003) J Proteins 50:451
20. Heine T et al. (1999) J Phys Chem A 103:8738
21. Bohr H et al. (1999) Chem Phys 246:13
22. Scholz R et al. (2000) Phys Rev B 61:13659
23. Witek H, Irle S, Morokuma K (2004) J Chem Phys 121:5171
24. Niehaus T et al. (2001) Phys Rev B 63:5108

25. Fabian J et al. (2002) J Mol Struc (THEOCHEM) 594:41
26. Wanko M et al. (2004) J Chem Phys 120:1674
27. Herringer D (2005) J Chem Phys (accepted)
28. Pecchia A, Di Carlo A (2004) Rep Prog Phys 67:1497
29. Chuang YY, Corchado JC, Truhlar DG (1999) J Phys Chem A 103:1140
30. Corchado JC, Espinosagarcia J, Rossi I, Truhlar DG (1995) J Phys Chem 99:687
31. Svensson M et al. (1996) J Phys Chem 100:96351
32. Cui Q, Guo H, Karplus M (2002) J Chem Phys 117:5617
33. Rossi I, Truhlar DG (1995) Chem Phys Lett 233:231
34. Niehaus T et al. (2001) J Mol Struc (THEOCHEM) 541:185
35. Elstner M et al. (2003) J Comput Chem 24:565
36. Elstner M (1998) Dissertation, University Paderborn
37. Krüger T, Elstner M, Schiffels P, Frauenheim T (2005) J Chem Phys 122:114110
38. Witek H, Morokuma K (2004) J Comp Chem 25:1858
39. Witek H, Irle S, Morokuma K (2004) J Chem Phys 121:5163
40. Soler JM et al. (2002) J Phys Condens Matter 14:2745
41. Lippert G, Hutter J, Parrinello M (1997) Mol Phys 92:477
42. Kalinowski JA et al. (2004) J Phys Chem A 108:2545
43. Dewar M, Thiel W (1977) J Am Chem Soc 99:4899
44. Elstner M et al. (2001) J Chem Phys 114:5149
45. Tang MS et al. (1996) Phys Rev B 53:979
46. Elstner M et al. (2000) Chem Phys 256:15
47. Elstner M et al. (2001) Chem Phys 263:203
48. Jalkaanen K, Elstner M, Suhai S (2004) J Mol Struc (THEOCHEM) 675:61
49. Shishkin OV et al. (2003) J Mol Struc (THEOCHEM) 625:295
50. Shiskin AV et al. (2003) Int J Mol Sci 4:537
51. Reha D et al. (2002) J Am Chem Soc 124:3366
52. Kumar A, Elstner M, Suhai S (2003) Int J Quant Chem 95:45
53. Kumar A et al. (2004) J Comp Chem 25:1047
54. Zhou H et al. (2002) J Mol Struc (THEOCHEM) 277:91
55. Sugihara M, Buss V, Entel P, Elstner M, Frauenheim T (2002) Biochemistry-US 41:15259
56. Wanko M et al. (2005) J Phys Chem B 109:3606
57. Okada T et al. (2004) J Mol Biol 342:571
58. Kristyan S, Pulay P (1994) Chem Phys Lett 229:175
59. Hobza P, Sponer J, Reschel T (1995) J Comp Chem 16:1315
60. Perez-Jorda JM, Becke AD (1995) Chem Phys Lett 233:134
61. Zhang Y, Pan W, Yang W (1997) J Chem Phys 107:7921
62. Perez-Jorda JM, San-Fabian E, Perez-Jiminez AJ (1999) J Chem Phys 110:1916
63. Wu X et al. (2001) J Chem Phys 115:8748
64. Johnson ER, Wolkow RA, DiLabio GA (2004) Chem Phys Lett 394:334
65. Wesolowski TW, Parisel O, Ellinger Y, Weber J (1997) J Phys Chem A 101:7818
66. Cybulski SM, Severson CE (2005) J Chem Phys 122:014117
67. Novoa JJ, Fuente P, Mota F (1998) Chem Phys Lett 290:519
68. Milet A, Korona T, Mozynski R, Kochanski E (1999) J Chem Phys 111:7727
69. Ireta J, Neugebauer J, Scheffler M (2004) J Phys Chem A 108:5692
70. Xu X, Goddard WA (2004) Proc Natl Acad Sci 101:2673
71. Kafafi SA (1998) J Phys Chem A 102:10404
72. Adamo C, Barone V (1998) J Chem Phys 108:664
73. Wu Q, Yang W (2002) J Chem Phys 116:515
74. Xu X, Goddard WA (2004) J Chem Phys 121:4068
75. Zhang Y, Yang W (1998) Phys Rev Lett 80:890
76. Rydberg et al. (2003) Phys Rev Lett 91:126402
77. Byrd EFC, Scuseria G, Chabalowski CF (2004) J Phys Chem B 108:13100
78. Kohn W, Meir Y, Makarov DE (1998) Phys Rev Lett 80:4153
79. Osinga VP, va Gisbergen SJA, Sniders JG, Baerends EJ (1997) J Chem Phys 106:5091
80. Hesselmann A, Jansen G, Schütz M (2005) J Chem Phys 122:014103
81. Hesselmann A, Jansen G (2003) Phys Chem Chem Phys 5:5010
82. Williams HL, Chabalowski CF (2001) J Phys Chem A 105:646
83. Langreth DC et al. (2005) Int J Quant Chem 101:599
84. Dobson JF et al. (2005) Int J Quant Chem 101:579
85. Ikura H, Tsuneda T, Hirao K (2001) J Chem Phys 115:3540
86. Hepburn J, Scolesc G, Penco R (1975) Chem Phys Lett 36:451
87. Gonzales C, Lim EC (2003) J Phys Chem 107:10105
88. Becke AD, Johnson ER (2005) J Chem Phys 122:154104
89. Johnson ER, Becke AD (2005) J Chem Phys 123:024101
90. Wu Q, Yang W (2002) J Chem Phys 116:515
91. Zimmerli U, Parrinello M, Koumoutsakos P (2004) J Chem Phys 120:2693
92. Grimme S (2004) J Comp Chem 25:1463
93. Cai Z-L, Sendt K, Reimers J (2002) J Chem Phys 117:5543
94. Grimme S, Parac M (2003) Chem Phys Chem 3:292
95. Dreuw A, Head-Gordon M (2004) J Am Chem Soc 126:4007–4016
96. Dreuw A, Head-Gordon M (2003) J Chem Phys 119:2943
97. Niehaus T et al. (2005) Phys Rev A 71:022508
98. Gritsenko O, Baerends EJ (2004) J Chem Phys 121:655
99. Yanai Y, Tew DP, Handy NC (2004) Chem Phys Lett 393:51
100. Koslowski A, Beck ME, Thiel W (2003) J Comput Chem 24:714
101. Neese F (2003) J Chem Phys 119:9428
102. Elstner M, Porezag D, Frauenheim Th, Suhai S, Seifert G (1999) Selfconsistent-charge density-functional tight-binding method for simulations of biological molecules. In: Multiscale Modelling of Materials. Mat Res Soc Symp Proc 538:243
103. Voituk AA, Bliznuk AA (1987) Theor Chim Acta 72:223
104. Jug K, Geudtner G (1993) J Comp Chem 14:639
105. Cui Q, Elstner M, Karplus M (2002) J Phys Chem B 106:2721
106. Zhang X, Harrison D, Cui Q (2002) J Am Chem Soc 124:14871
107. Li G, Cui Q (2003) J Am Chem Soc 125:15028
108. Smedarchina S et al. (2003) J Am Chem Soc 125:243
109. Meuwly M, Karplus M (2002) J Chem Phys 116:2572
110. Zoete V, Meuwly M (2004) J Chem Phys 121:4377
111. Bondar N et al. (2004) Structure 12:1281
112. Bondar N et al. (2004) J Am Chem Soc 44:14668
113. Walewski L et al. (2004) Chem Phys Lett 397:451
114. Barone V, Adamo C (1996) J Chem Phys 105:11007
115. Sadhukan et al. (1999) Chem Phys Lett 306:83
116. Gao J, Truhlar D (2002) Ann Rev Phys Chem 53:467
117. Smith B, Radom L (1994) Chem Phys Lett 231:345
118. Curtiss LA et al. (2000) J Chem Phys 112:7374
119. Range K et al. (2005) Phys Chem Chem Phys 7:3070
120. Reynolds CH (1997) J Mol Struc (THEOMCHEM) 401:267